JOURNAL OF OPTOELECTRONICS AND ADVANCED MATERIALS Vol. 10, No. 3, March 2008, p. 623 - 627

Holographic images of a spark channel generated on the optical wedge surfaces

M. MIHĂILESCU*, L. PREDA, A. PREDA, E. SCARLAT
"POLITEHNICA" University of Bucharest, Department of Physics I, 313 Splaiul independenţei , 060042 – Bucharest, Romania

In this paper, we present an application of digital holography for the characterization of a SC produced in atmospheric air by a point-point spark gap located between surfaces of an air wedge. This air wedge is obtained using two glass wedges having two wire electrodes situated along the diagonal of glass plates, between their adjacent surfaces. The experimental setup used for power supply of spark gap is built from an saturable transformer. One divergent laser beam passes through this optical system and produces two holographic images (interference images): one obtained from the reflections on the surfaces of the wedges (the hologram) and one from the transmitted beam (the shadowgram). The holographic images are recorded using a CCD camera and computer processed in order to extract the amplitude and the phase corresponding to every image pixel. The holographic and shadowgrapic images are processed with 2D Fourier transform using phase map and fractional correlation.

(Received September 25, 2007; accepted March 12, 2008)

Keywords: Spark channel, Digital holography, Shadowgram, Fractional correlation

1. Introduction

In the past time, the spark channel (SC) at the atmospheric pressure, is of the significant interest for: laser physics [1], deposition of thin film [2], surface treatment [3], and for pollution control [4]. In this paper, we apply the digital holography for the characterization of the modification of the surface of the optical plate in contact with a SC produced by a point-point spark gap.

It is possible to define a SC as a class of transient occurrences in which a given existing conduction current in a gas suddenly and irreversibly change to a current of a higher magnitude, operating more efficiently by a different mechanism under the imposed condition which rendered the lower current unstable. The SC is formed from many streamers which are transient filamentary plasmas whose dynamics are controlled by highly localized non-linear space-charge waves [5].

The digital holographic method offers many advantages over other techniques for testing of surface shape, flatness, homogeneity of optical glass as well as pulsed plasmas [6]. Starting with one hologram recorded on CCD, we can numerically reconstruct, using Fresnel transform, the amplitude and the phase of the real objects. The phase map, is used to characterize different depth of the object, from one hologram without scanning in z direction.

2. Experimental setup

Electrical setup is schematically shown in Fig. 1. A spark gap (SP1) was used both for charging the capacitor C=1nF from saturable transformer (TRS) and for discharging it to spark gap SP2.

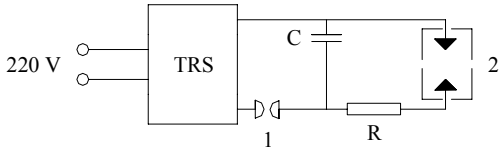

Fig. 1. Electrical setup

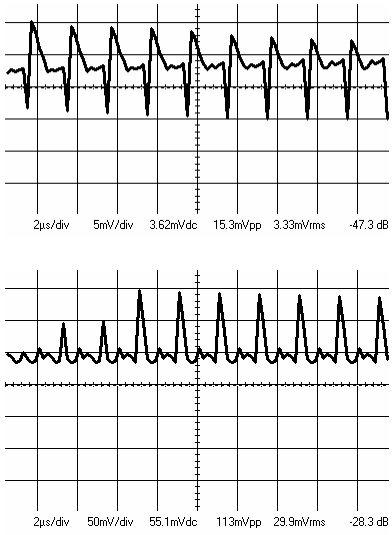

Fig. 2. Typical voltage (a) and current (b) oscilogrames.

The pulse repetition rate was controlled by SP1. By adding dumping resistor R, the voltage pulse rise rate could be modified. The voltage pulse and discharge current was measured and recorded with a digital oscilloscope. When the SC develops, a complex current

waveshape is observed. Typical voltage and current oscilogram are shown in Fig. 2.a) and 2b). The peak voltage from TRS is 25kV and the peak current in SC is 10A.

Fig. 3 sown the optical arrangement of the holographic and shadowgraphic system proposed here. A He-Ne Laser (S) is focalized in point F by lens L and gaussian beam have a divergence at incidence on the two wedges (P1 and P2). Between P1 and P2 is produced the SC. The images from this optical system are recorded on a CCD in the planes E (shadowgram) and H (hologram). The plane H and E are situated at 8 m distance from F. Images from these two planes are recorded on a CCD detector.

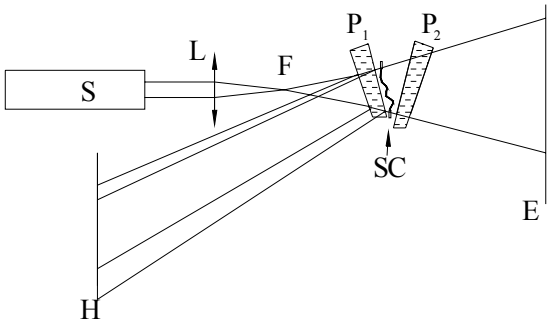

Fig. 3. The optical setup.

3. Theory

The image of F is formed in two different points F1 and F2 from the surface (1) and (2) of wedge P_1 (Fig. 4.). In the H plane we have two gaussian beams which interfere to form the hologram (H_R) of the reference surface in the first case when the SC is absent. In the second case, the surface (2) of P1 is modified by SC and form in H plane, the hologram (H_O) of the modified surface. Similarly work the wedge P_2.

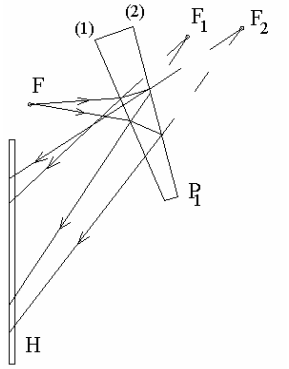

Fig. 4. The optical path of the beam from P_1 which interfere in H plane.

H_R was obtained from superimposed of two Gaussian beams form P_1 without SC:

$$u_{Rj}(x,y,z_j) = \\ = A\frac{w_0}{w_j}\exp\left[i\left(kz_j+\Phi_j(z_j)\right)-\frac{ik}{2q_j}\left(x^2+y^2\right)\right], \quad \text{j=1,2} \tag{1}$$

where A is a constant, w_0 is beam waist in F where z=0 (Fig. 4.), and

$$w_j^2(z_j) = w_0^2\left[1+\left(\frac{2z_j}{kw_0^2}\right)^2\right] \tag{2}$$

is the radial dimension of the beam at distance z from waist, $k = 2\pi/\lambda$ the wave number, the phase

$$\Phi_j(z_j) = \tan^{-1}\left(\frac{kw_0^2}{2z_j}\right). \tag{3}$$

The complex parameter q_j of one Gaussian beam, is given by:

$$\frac{1}{q_j} = \frac{1}{R_j(z_j)} - \frac{2i}{kw_j^2(z_j)} \tag{4}$$

where $R_j(z_j) = z_j\left[1+\left(\frac{w_0^2k}{2z_j}\right)^2\right]$ (5)

is curvature ray of the wave front. $\Delta z = z_2 - z_1 = 2d$ equal with distance between F_1 and F_2 and d is the thickness of the wedge in the z axis.

When SC appear, the Gaussian beam u_{R2} will be transformed in u_O due to SC influence. In H plane we have the intensity distributions will be:

$$I_R \approx \left(u_{R1}+u_{R2}\right)\left(u_{R1}^*+u_{R2}^*\right) \tag{6}$$

of the H_R without SC and

$$I_O \approx \left(u_{R1}+u_O\right)\left(u_{R1}^*+u_O^*\right) \tag{7}$$

of the H_O with SC. HR and HO are numerically processing to give us information about the modified surface by SC. In E plane, are obtained the projection of the two wedge assembly (in case one) or two wedge assembly with SC (in case two), in which we have information about the phase map and the amplitude map from SC.

For shadowgraphic plane, we simulated two situations: the SC in two different moments, and we made the correlation map of order k between them [8]:

$$C_{R,O}^{k} = \left| O_1 \underset{k}{\otimes} O_2 \right|^2 = \tag{8}$$
$$= \left| \mathcal{F}^{-1} \left[\left| \tilde{O}_1 \right|^k \exp(i\varphi_1) \left| \tilde{O}_2 \right|^k \exp(-i\varphi_2) \right] \right|^{-1}$$

where $O_1(x,y,t_1)$ is reference shadowgram at moment t_1 with SC and $O_2(x,y,t_2)$ is the shadowgram at moment t_2, $\tilde{O}_1, \tilde{O}_2$ are their Fourier transform with amplitude $\left|\tilde{O}_1\right|, \left|\tilde{O}_2\right|$ and phase φ_1, φ_2 in object plane.

4. Simulation

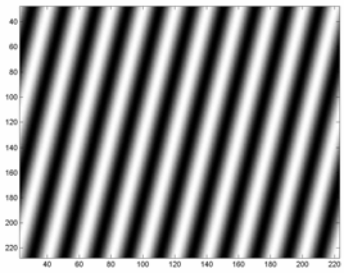

a)

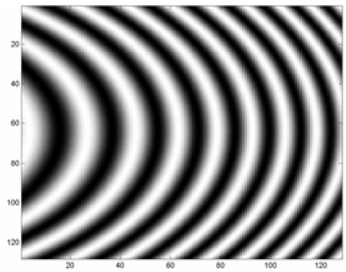

b)

Fig. 5. Simulated holograms.

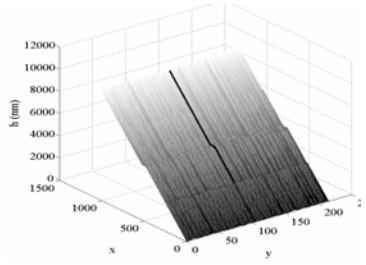

a)

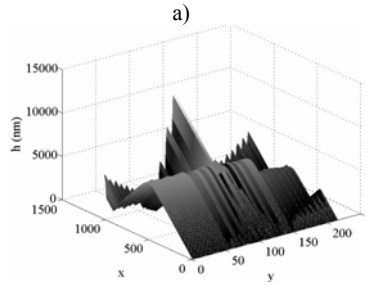

b)

Fig. 6. The depth in object plane starting with holograms from Fig. 5.

We generated two holograms similarly with the experimental one H_R and H_O, like in Fig. 5a and b. We simulate the back propagation, using 2D Fourier transform, in order to obtain the phase $\varphi_H(x,y)$ and amplitude maps of the modified surface [7]. The firs simulated hologram represents I_R, and the second is I_O. The depth of the surface in every point,

$$h(x,y) = \frac{\lambda \varphi_H(x,y)}{4\pi \cdot n}, \tag{9}$$

was calculated from unwrap phase map in object plane starting with I_R, (Fig. 6a) and I_O, (Fig. 6b). Here n is the refractive index of the glasses, which P1 is made from. The numbers in Fig. 6, on x and y axes are the number of pixels.

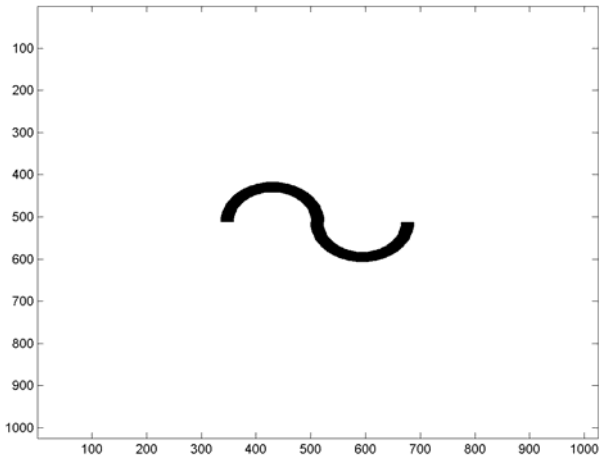

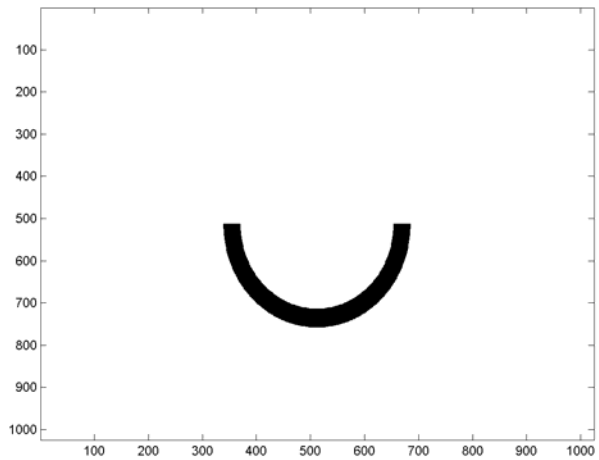

Fig. 7 Two simulated shapes of SC in E plane.

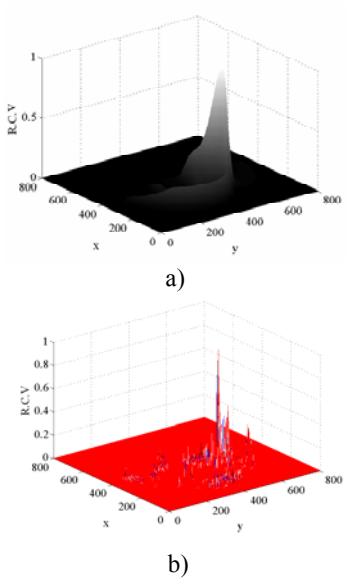

Fig. 8. The relative correlation value in normalized units for k=1 (classical correlation) and fractional correlation k=0.2 starting with images from Fig. 7.

5. Experimental results

In Fig. 9 a) and b) are the experimental holograms with intensity distribution given by I_R and respectively I_O. The simulated back propagation using 2D Fourier transform, gives us information about complex shape of the object. This object is formed from the deformation of the surface (2) of P_1 and SC. In Fig. 9b) we observe the displacement of the fringes and the intensity increases along the crooked spark channel.

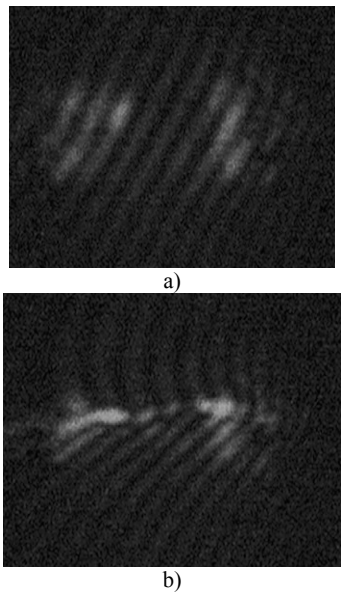

Fig. 9. a) Experimental reference hologram; b) experimental hologram with SC in object plane.

In Fig. 10, we present the fractional correlation of order k=0.2 between holograms from Fig. 9. The region where the relative correlation value has nonzero values, is linked to the surface (2) deformation of wedge P1.

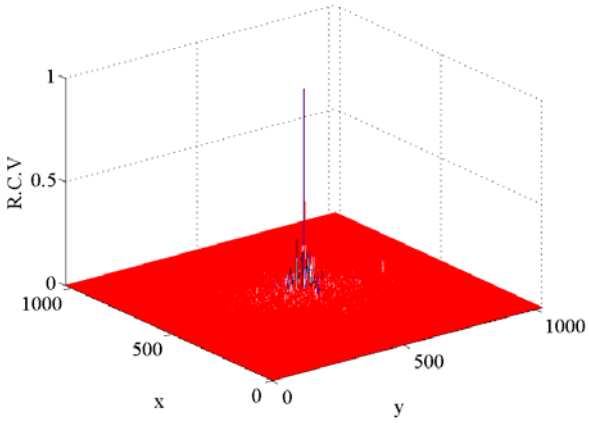

Fig. 10 The fractional correlation of order k=0.2 between holograms from Fig. 9.

The shadowgrams of the crooked spark channel in E plane at two different moments is in Fig. 11. The black regions are the two electrodes and the in brightness regions are the crooked spark channel. The difference between these two shadowgrams, we expressed with the similarity criterion given by the fractional correlation with k=0.2 (Fig. 12). We observed that we have a nonzero values in the direction of crooked spark channel. This conclusion is based on the simulations presented in Fig. 8.

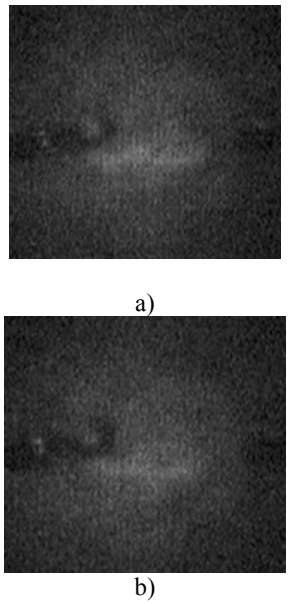

Fig. 11 Experimental shadowgrams at two different moments at 0.5s

In E plane, we simulated two shapes of SC (Fig. 7a and b). In Fig. 8a is correlation map calculated like in

classical Fourier optics [9] (k=1). In Fig. 8b is the fractional correlation map of order k=0.2 (eq. 8). In this way, we relief the zone where the SC is modified in time. We observe that in the case of fractionar correlation, we improves the discrimination between similar objects. We use a *k*-th fractional correlation with *k*= 0.2 because we have found that this value of *k* provides the best discrimination capability.

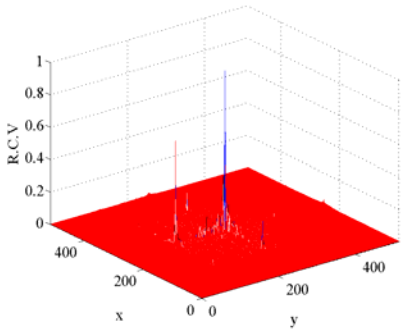

Fig. 12 The fractional correlation of order k=0.2 between shadowgrams from Fig. 11.

6. Conclusions

We present an experimental setup to generation and to study the characteristics parameters of the discharge plasma at the atmospheric pressure on the optical components. This study was made with the digital holographic methods in real and Fourier plane based on phase maps. The simulations linked with this spark gap help us to selection and processing the information from experimental holograms and shadowgrams. Our method aloud us to obtain information about the spatial and temporal evolution of the crooked spark channel.

The holograms give us information about the deformations induced by SC, and the shadowgrams give information about crooked spark channel. The brightness of the crooked spark channel in shadowgrams shows that the spark gap action like a cylindrical convergent lens for incident light and can be modeled like a phase object.

References

[1] A. N. Tkachev, S. I. Yakovlenco, Laser Physics **17**(1), 5-11 (2007).
[2] P. Fauchais, R. Etchart-Salas, C. Delbos, M. Tognonvi, V. Rat, J. F. Coudert, T. Chartier, J. Phys. D Appl. Phys. **40**, 2394, (2007).
[3] Z. Falkenstein, J. J. Coogan, J. Appl. Phys. **8**, 6273 (1997).
[4] G. G. Xia, J. Y. Wang, A. Huang, S. L. Suib, Rev. of Sci. Instrum **72**(2), 1383 (2001).
[5] P. A. Vitello, B. M. Penetrante, J. N. Bardsley, Phys. Rev. E **49**(6), 5574 (1994).
[6] O. K. Ersoy, Diffraction, Fourier Optics and Imaging, Wiley-Interscience, John Wiley & Sons, Inc. Publication, 2007. M.Mihailescu, Doctoral thesis, 2007.
[7] Y. Frauel, E. Tajahuerce, O. Matoba, A. Castro, B. Javidi, Appl. Opt. **43**(2), 452 (2004).
[8] J. W Goodman, Introduction to Fourier Optics, Mc Graw-Hill Book Company, 1968.

*Corresponding author: mona_m@physics.pub.ro